OPTOELECTRONICS AND ADVANCED MATERIALS – RAPID COMMUNICATIONS Vol. 12, No. 7-8, July-August 2018, p. 413 - 416

Investigation of electrical and structural properties of In-doped CdTe/CdS thin-film solar cells produced by E-beam techniques

I. KIRBAS[a,*], R. KARABACAK[b], K. YILMAZ[c], D. TAKANOGLU[c]
[a]*Mehmet Akif Ersoy University Vocational School of Technical Sciences, 15100 Burdur, Turkey*
[b]*Pamukkale University, Engineering Faculty, Mechanical Engineering Department, 20070 Denizli, Turkey*
[c]*Pamukkale University, Arts and Science Faculty, Department of Physics, 20020 Denizli, Turkey*

In the current study, the electron beam (e-beam) evaporation deposition technique was utilized to examine the effect of annealing on the structural and electrical properties of In-doped CdTe/CdS thin-film solar cells. Thin-film solar cells were deposited onto the ITO-coated glass substrate with the e-beam technique. These solar cells were characterized by X-ray diffraction (XRD), scanning electron microscopy (SEM), and energy dispersive X-ray (EDS) analysis. The crystallite size, inter-planer distance, and lattice constant values were calculated for the thin-film solar cells using XRD data. The current–voltage (I–V) characteristics of the solar cells were examined by solar simulator.

(Received March 14, 2017; accepted August 9, 2018)

Keywords: Thin-film solar cells, E-beam, In-doped CdTe, Structural properties, Electrical properties

1. Introduction

CdTe thin films are a semiconductor that finds applications in solar energy conversion, X-ray and gamma detectors, electro-optic modulators, photoconductive devices, and the medical, defence, and security industries [1, 2] due to their low thermal noise and high absorption coefficient [3, 4]. CdTe II–VI compound semiconductors and the 1.5 eV band range are very suitable for photovoltaic applications [5]. Some recent studies report that CdTe/CdS solar cells are highly efficient [6].

Doping is a phenomenon that is studied extensively in order to obtain electron hole conductivity in semiconducting materials. A considerable reduction in the cost of the devices can be achieved by preparing polycrystalline thin films with appropriate quality. In polycrystalline semiconductor films, doping is often difficult and new technologies need to be developed. The deposition of polycrystalline semiconductor films using electron beam techniques is thought to be much more economical than deposition of thin layers by techniques such as molecular beam epitaxy. Both low- and high-resistivity materials can be obtained by using various amounts of Indium as dopant in CdTe [7].

In this article, In-doped CdTe was used as the absorber layer and CdS was used as the window layer to form an In-doped CdTe/CdS thin-film solar cell structure. The structural and electrical properties of the solar cells obtained and the effect of annealing on these properties was investigated. The results are presented in graphs and tables.

2. Materials and methods

Powdered Cd, Te and In were sintered to obtain polycrystalline In-doped CdTe. For sintering; For CdTe prepared by weighing at stoichiometric ratios, 8 g of Cd was added to 9.08 g of Te and 0.17 g of In was added to doped 1% of In. These materials were placed on quartz tubes and the mouths of the tubes were closed. The sintering process was started by placing the tubes in a horizontal furnace. The oven was gradually heated. When the oven temperature reached 1150 o C after 48 hours, it was left for 24 hours. After the crystal formation was achieved, the cooling process was carried out gradually. The obtained polycrystalline material was powdered again.

ITO-coated glass substrate by e-beam system after being placed on the retention of graphite crucibles of polycrystalline materials (In-doped CdTe) in powder form was placed in a water-cooled crucible cabin. The storage process was started when the e-beam system reached the required vacuum value. First, substrate rotation was commissioned in order to obtain film homogeneity. The process was started by applying a current of 2 mA. The evaporation rate during storage was kept at approximately 10–12 Å/s. The system automatically ended the storage process when the thickness was 0.7 μm by turning off the circuit breaker. In-doped CdTe deposited substrates were annealed for 1 hour in a horizontal furnace heated up to 400 °C and maintained in a nitrogen atmosphere [8]. The absorber structure was formed, and annealed (E1_400) and as-deposited (E1) samples were reseated in the e-beam system. Then the CdS (99.999% pure) was placed into a graphite crucible in the system, which was closed. The deposition started when the vacuum value was 2×10^{-5}

Torr and the process was continued until the thickness was 0.7 µm. After the window layer structure was formed, indium contacts were deposited on annealed and as-deposited samples.

The surface morphology and compositions of films were examined by scanning electron microscopy (SEM) and energy dispersive X-ray spectroscopy (EDS) analysis with a Quanta (FEG-250) model. The crystal structure of semiconductor films was investigated by X-ray diffraction (XRD) measurements taken using a Bruker XRD system (D8 Advance). The current–voltage (I–V) characteristics of the solar cells were examined by solar simulator at room temperature.

3. Results and discussion

3.1. Structural analysis

An In-doped CdTe/CdS thin-film solar cell was deposited by the e-beam technique. E1 for the as-deposited In-doped CdTe layer and E1_400 for the annealed In-doped CdTe layer. The XRD diffractions of E1 and E1_400 thin-film solar cells were shown in the Fig. 1. The positions of the peaks of the E1 and E1_400 samples were observed to be at approximately 2θ = 23.9°, 26.6°, and 33.0°. These peaks corresponded, respectively, to the diffraction lines produced by the (111), (200), and (211) crystalline planes. When the peaks obtained were examined, it was determined that the intensity increased due to the annealing. Annealing helped to eliminate structural defects. At the same time, it enabled the thin films to pass from an amorphous structure to a polycrystalline structure [9].

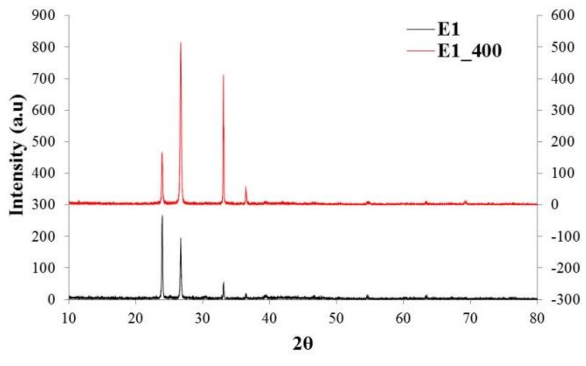

Fig. 1. The X-ray diffraction patterns of the absorber layer of E1 and E1_400 thin-film solar cells

The crystallite sizes of thin films were calculated with XRD data using the Scherrer formula [10]:

$$D = \frac{k\lambda}{\beta Cos\ \theta}$$

where D is the crystal size, λ is the wavelength of the X-ray source, β is half of the maximum width of the diffraction peak in radians, θ is the Bragg angle of XRD peak, and k is a constant related to the film whose particle size is being calculated [10].

The lattice constant (a) for cubic samples was calculated using the relation: $a = d(h^2 + k^2 + l^2)^{0.5}$, where h, k, and l are the lattice planes and (d) is the inter-planar distance, measured using the Bragg equation [11]. The values for E1 and E1_400 calculated for thin film solar cells are given in Table 1. It was determined that the crystallite size increased due to the effect of the annealing. The increased crystallite size was an indication that the films had changed from an amorphous structure to a polycrystalline structure.

Table 1. Inter-planar distance (d), lattice constant (a), and crystallite size (D) of E1 and E1_400 samples

	hkl	2θ °	*d* (Å)	*a* (Å)	*D* (nm)
E1	(111)[a]	23.91	3.717	6.438	30.30
	(200)[b]	26.68	3.337	6.674	24.36
	(211)	33.04	2.707	6.631	24.05
E1_400	(111)[a]	23.89	3.720	6.443	38.56
	(200)[b]	26.69	3.336	6.672	32.83
	(211)	33.04	2.707	6.633	29.86

[a] Ref. [5] [b] Ref. [12]

3.2. Surface morphology analysis

In order to determine the morphology of the surface material for annealed and as-deposited solar cells, SEM images of the absorber layer are shown in Fig. 2. Flocculation, surface roughness, and the crystallite size on the film surface can be seen in Fig. 2a. It was determined that the annealing had the effect of decreasing the surface roughness and agglomeration while increasing the crystallite size in the film (Fig. 2b).

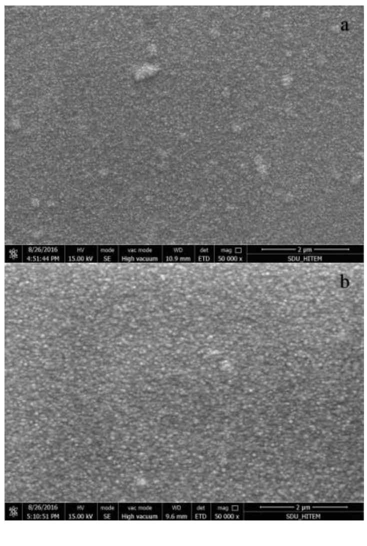

Fig. 2. SEM images of absorber layer: (a) E1 and (b) E1_400

3.3. Composition analysis

The energy dispersive X-ray (EDS) spectra of the annealed and as-deposited samples are shown in Fig. 3.

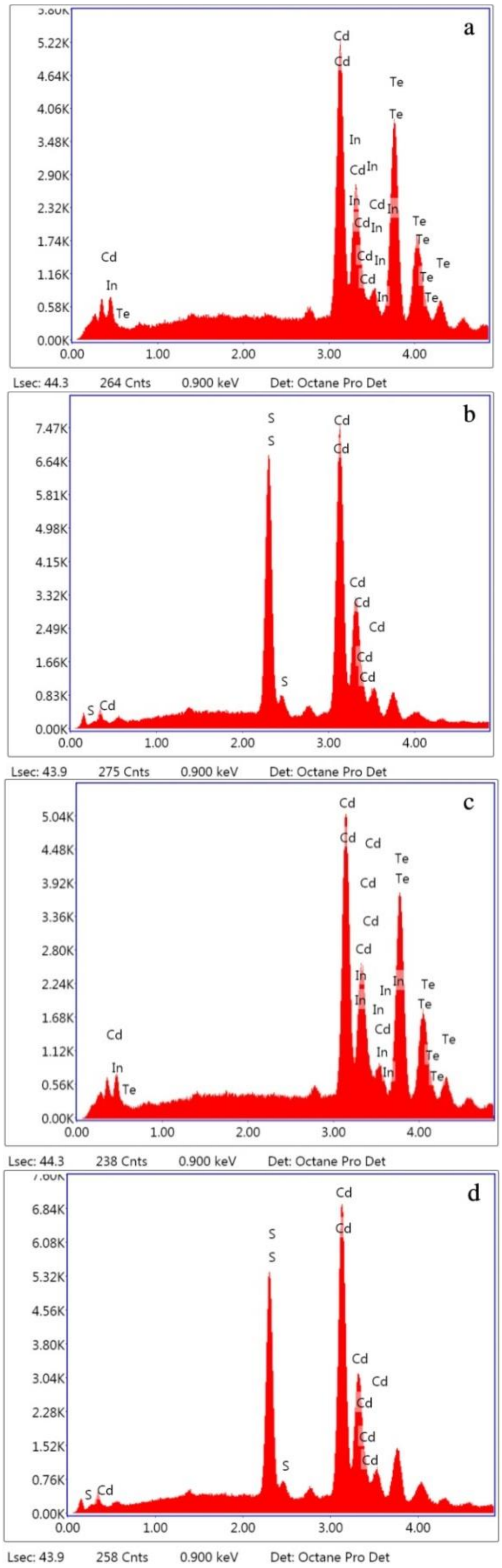

Fig. 3. Energy dispersive X-ray (EDS) spectra taken for E1: (a) In-doped CdTe layer, (b) CdS layer; and E1_400: (c) In-doped CdTe layer, (d) CdS layer

The EDS analysis results for the deposited thin-film solar cells are shown in Table 2. An increase in the In and Te ratios and a decrease in the Cd ratio were observed in the deposited absorber layer obtained by the e-beam evaporation technique after annealing.

Table 2. EDS results of the absorber layer (In-doped CdTe layer) and the window layer (CdS)

	E1		E1_400	
Elements	**Average weight %**	**Atomic weight %**	**Average weight %**	**Atomic weight %**
Cd	41.00	43.93	40.49	43.39
In	3.70	3.88	4.10	4.30
Te	55.30	52.19	55.41	52.31
Cd	77.83	50.03	80.67	54.34
S	22.18	49.97	19.33	45.66

3.4. Electrical analysis

The dark and illuminated I–V characteristics of as-deposited and annealed In-doped CdTe/CdS thin-film solar cells are presented in Figs. 4 and 5. It is clearly visible in Fig. 4 that the variation in current with voltage for as-deposited and annealed In-doped CdTe/CdS thin films solar cells was continuous. It is observed that the current of the solar cells is increased for annealed solar cells. The annealed solar cell shows ideal diode characteristics. Also, it is observed that the highest forward and reverse current at constant voltage can be obtained for annealed solar cells, indicating their high conductivity. The results are consistent with previous work [13]. The illuminated I-V variations showed that the sensitivity to light increased for the annealed cell (Fig. 5) for which efficiency was determined slightly under 1%.

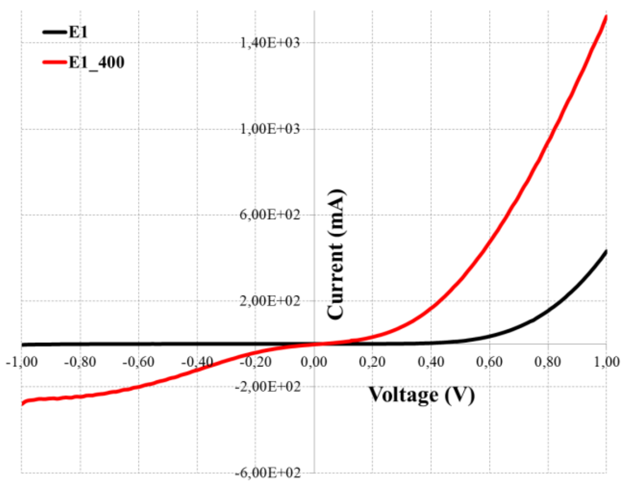

Fig. 4. E1 and E1_400 In-doped CdTe/CdS thin-film solar cells dark I–V characteristics

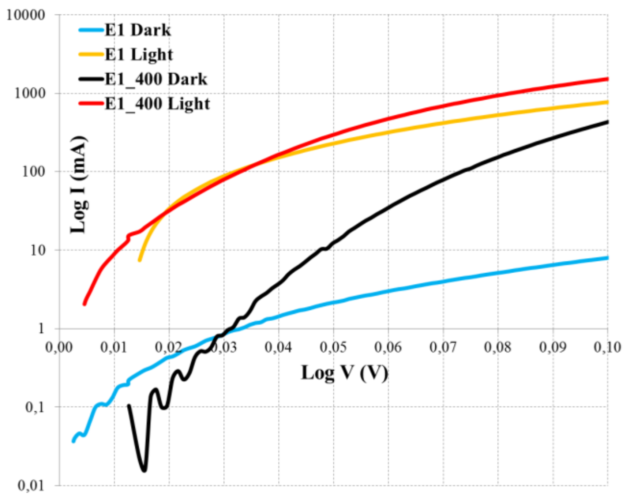

Fig. 5. E1 and E1_400 In-doped CdTe/CdS thin-film solar cells illuminated I–V characteristics

4. Conclusion

The e-beam technique was used to fabricate p-In-doped CdTe and n-CdS structures on an ITO-coated glass substrate. Both annealed and as-deposited thin-film solar cells were investigated to determine their structural and electrical properties. Through XRD analysis, as-deposited and annealed solar cells were found to be in the (111), (200), and (211) crystal directions. The positions of the largest peaks were found to be at $2\theta = 23.9^o$, 26.6^o and 33.0^o for as-deposited and annealed solar cells respectively. Particle size was also calculated; annealed films were found to have increased particle size, indicating clearly that a polycrystalline structure has been formed. In addition, the inter-planar distance (d) and lattice constant (a) values were calculated using Bragg's law. SEM and EDS analyses showed an increase in surface roughness and a decrease agglomeration of the annealed solar cells, and no impurity atoms were found in the structure. The I–V characteristics showed that the current and the sensitivity to light increased for annealed thin-film solar cells.

Acknowledgements

This work was financially supported by the Scientific Research Projects Center (BAP) of Pamukkale University (project number: 2014FBE007). SEM, EDS and solar simulator analysis were performed in the HITEM laboratory of Süleyman Demirel University.

References

[1] P. Fochuk, et al., Journal of Crystal Growth **207**, 273 (1999).
[2] J. Zázvorka, P. Hlídek, R. Grill, J. Franc, E. Belas, Journal of Luminescence **177**, 71 (2016).
[3] M. S. Han, B. K. Song, Y. B. Hou, T. W. Kang, T. W. Kim, Applied Surface Science **119**, 219 (1997).
[4] Sh. U. Yuldashev, et al., Solid State Communications **110**, 413 (1999).
[5] M. Becerril, et al., Journal of Physics and Chemistry of Solids **60**, 257 (1999).
[6] T. Ganetsos, Procedia Engineering **25**, 354 (2011).
[7] P. Fochuk, et al., Journal of Alloys and Compounds **664**, 499 (2016).
[8] B. V. Rajendra, D. Kekuda, J. Mater. Sci.: Mater. Electron. **23**, 1805 (2012).
[9] M. Singsangah, et al., Journal of Colloid and Interface Science **451**, 189 (2015).
[10] M. M. El-Nahass, G. M. Youssef, S. Z. Noby, Journal of Alloys and Compounds **604**, 253 (2014).
[11] A. Y. Shenouda, M. M. Rashad, L. Chow, Journal of Alloys and Compounds **563**, 39 (2013).
[12] S. Singh, R. Kumar, K. N. Sood, Thin Solid Films **519**(3), 1078 (2010).
[13] W. F. Mohammed, M. A. S. Yousif, Renewable Energy **26**, 285 (2002).

*Corresponding author: ikirbas@mehmetakif.edu.tr